

**Electronic Supporting Information**

**Cross-linked supramolecular polymer  
metallogels constructed via self-sorting strategy  
and their multiple stimuli-responsive behaviors**

Xu-Qing Wang,<sup>a</sup> Wei Wang,<sup>a</sup> Guang-Qiang Yin,<sup>a</sup> Yu-Xuan Wang,<sup>a</sup> Chang-Wei Zhang,<sup>a</sup>

Jia-Meng Shi<sup>b</sup>, Yihua Yu,<sup>b</sup> and Hai-Bo Yang<sup>\*a</sup>

<sup>a</sup>Shanghai Key Laboratory of Green Chemistry and Chemical Processes, Department of Chemistry, EastChina Normal University, Shanghai 200062, P. R. China.

<sup>b</sup>Shanghai Key Laboratory of Magnetic Resonance, Department of Physics, East China Normal University, Shanghai 200062, P. R. China.

Fax: (+86) 21 -6223-5137 E-mail: [hbyang@chem.ecnu.edu.cn](mailto:hbyang@chem.ecnu.edu.cn)

## **Table of contents:**

<b>Electronic Supporting Information .....</b>	<b>1</b>
<b>1. General information .....</b>	<b>3</b>
<b>2. Experimental details for synthesis and characterization of guest 4 .....</b>	<b>4</b>
<b>3. Experimental details of Size-Controlled Self-Sorting Process.....</b>	<b>7</b>
<b>4. The construction and characterization of cross-linked supramolecular polymers through self-sorting complexation .....</b>	<b>8</b>
<b>5. Stimuli-responsive supramolecular polymer gels .....</b>	<b>17</b>

## 1. General information

The 120° benzo-21-crown-7 (**B21C7**)-containing host **1**<sup>1</sup>, 120° dibenzo-24-crown-8 (**DB24C8**)-containing host **2**<sup>2</sup>, organoplatinum 120° acceptor **3**<sup>3</sup> and compound **S1**<sup>4</sup> were prepared as the reported procedure. All reagents were of analytical purity and used without further treatment. TLC analyses were performed on silica-gel plates, and flash chromatography was conducted using silica-gel column packages purchased from Qingdao Haiyang Chemical Co., Ltd. (China).

<sup>1</sup>H NMR, <sup>13</sup>C NMR and <sup>31</sup>P NMR spectra were recorded on Bruker 400 MHz Spectrometer (<sup>1</sup>H: 400 MHz; <sup>13</sup>C: 100 MHz; <sup>31</sup>P: 161.9 MHz) and Bruker 500 MHz Spectrometer (<sup>1</sup>H: 500 MHz) at 298 K. The <sup>1</sup>H and <sup>13</sup>C NMR chemical shifts are reported relative to residual solvent signals. Coupling constants (*J*) are denoted in Hz and chemical shifts ( $\delta$ ) in ppm. Multiplicities are denoted as follows: s = singlet, d = doublet, m = multiplet, br = broad. 2D DOSY were recorded on Bruker 500 MHz Spectrometer (<sup>1</sup>H: 500 MHz) at 298 K.

**Dynamic Light Scattering (DLS) Studies.** DLS measurements were performed under a Malvern Zetasizer Nano-ZS light scattering apparatus (Malvern Instruments, U.K.) with a He-Ne laser (633 nm, 4 mW).

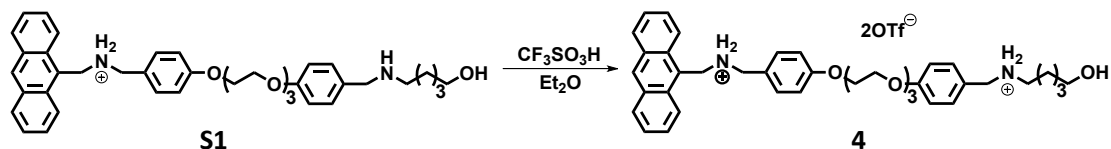
**Scanning Electron Microscopy (SEM) Experiments.** The SEM samples were prepared on clean Si substrates. To minimize sample charging, a thin layer of Au was deposited onto the samples before SEM examination. All the SEM images were obtained using a S-4800 (Hitachi Ltd.) with an accelerating voltage of 3.0-10.0 kV.

**Transmission electron microscopy (TEM) Experiments.** The TEM samples were deposited on copper grids, followed by a slow evaporation in air at room temperature. All the TEM measurements were performed under a Tecnai G2 20 TWIN device.

**Rheological Experiments.** Rheological measurements were performed under a MARS III (HAAKE MARS III) device at 293K.

## 2. Experimental details for synthesis and characterization of guest 4

**Scheme S1.** The synthetic procedure for the divalent guest **4**.



**Synthesis of guest 4.** **S1** (200 mg, 0.314 mmol) was added to diethyl ether (~10 mL) at room temperature. Trifluoromethanesulfonic acid (94.3mg, 0.628 mmol) was added to the stirred solution. A white precipitate was immediately observed, collected via vacuum filtration, washed with diethyl ether, and dried to give **4** as a pale yellow solid (245mg, 83%). M.p. 62 °C.  $^1\text{H}$  NMR (400 MHz,  $\text{CD}_3\text{CN}$ ):  $\delta$  8.76 (s, 1H),  $\delta$  8.17-8.19 (d,  $J = 8.0$  Hz, 2H),  $\delta$  8.09-8.11 (d,  $J = 8.0$  Hz, 2H),  $\delta$  7.59-7.69 (m, 4H),  $\delta$  7.51-7.53 (d,  $J = 8.0$  Hz, 2H),  $\delta$  7.36-7.39 (d,  $J = 12.0$  Hz, 2H),  $\delta$  7.06-7.08 (d,  $J = 8.0$  Hz, 2H),  $\delta$  6.97-6.99 (d,  $J = 8.0$  Hz, 2H),  $\delta$  6.86 (s, 1H),  $\delta$  5.22-5.25 (t,  $J = 12.0$  Hz, 2H),  $\delta$  4.45-4.48 (t,  $J = 12.0$  Hz, 2H),  $\delta$  4.07-4.19 (m, 4H),  $\delta$  3.79-3.84 (m, 4H),  $\delta$  3.68 (s, 4H),  $\delta$  3.41-3.50 (m, 4H),  $\delta$  3.00 (m, 2H),  $\delta$  1.63-1.69 (m, 2H),  $\delta$  1.45-1.51 (m, 2H),  $\delta$  1.36-1.42 (m, 2H).  $^{13}\text{C}$  NMR ( $\text{CD}_3\text{CN}$ , 100MHz):  $\delta$  160.44, 159.92, 133.29, 132.35, 132.05, 131.86, 131.26, 129.92, 127.62, 126.09, 124.35, 123.46, 115.50, 115.48, 71.06, 69.97, 69.89, 68.29, 68.25, 61.74, 52.70, 51.56, 48.12, 43.97, 32.14, 25.94, 23.12. HRMS (ESI): Exact mass calcd. for  $[\text{C}_{40}\text{H}_{49}\text{N}_2\text{O}_5]^+$  ( $[\text{M}-\text{OTf}-\text{HOTf}]^+$ ): 637.3636, Found: 637.3676.

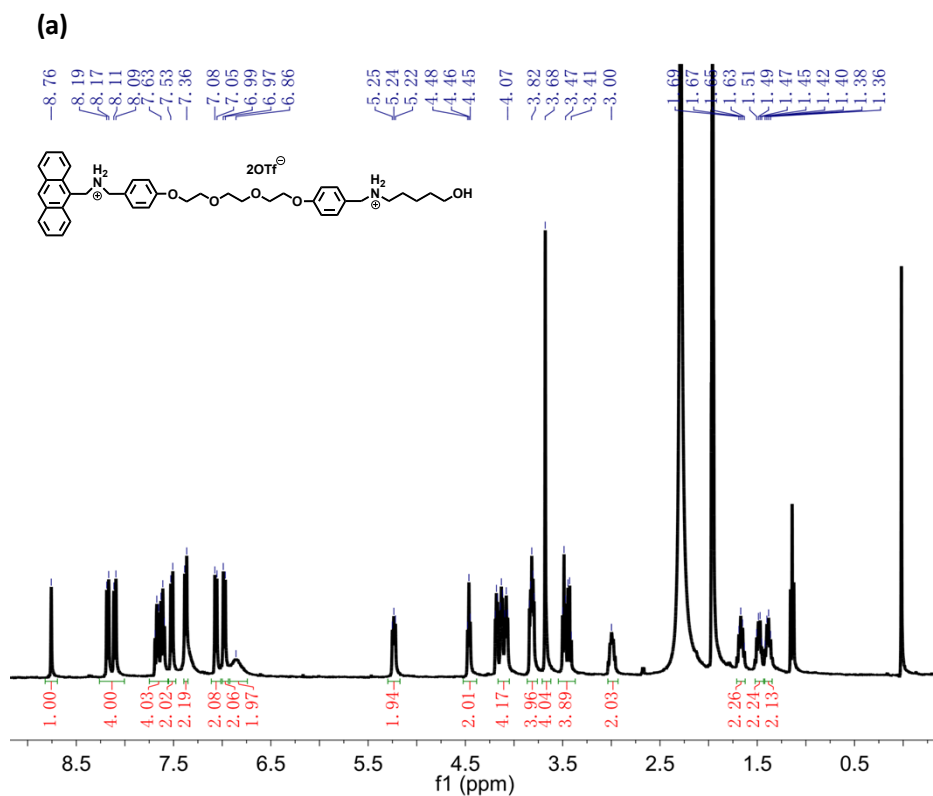


Fig. S1  $^1\text{H}$ NMR (400 MHz,  $\text{CD}_3\text{CN}$ , 298K) spectrum of guest 4.

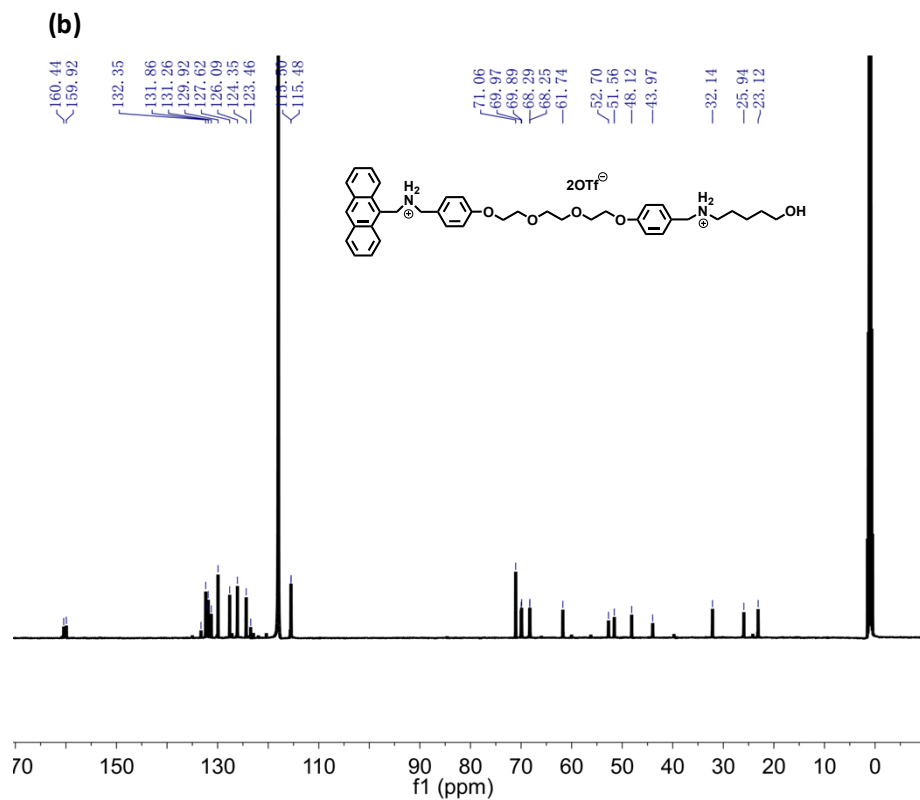


Fig. S2  $^{13}\text{C}$  NMR (100 MHz,  $\text{CD}_3\text{CN}$ , 298K) spectrum of guest 4.

(c)

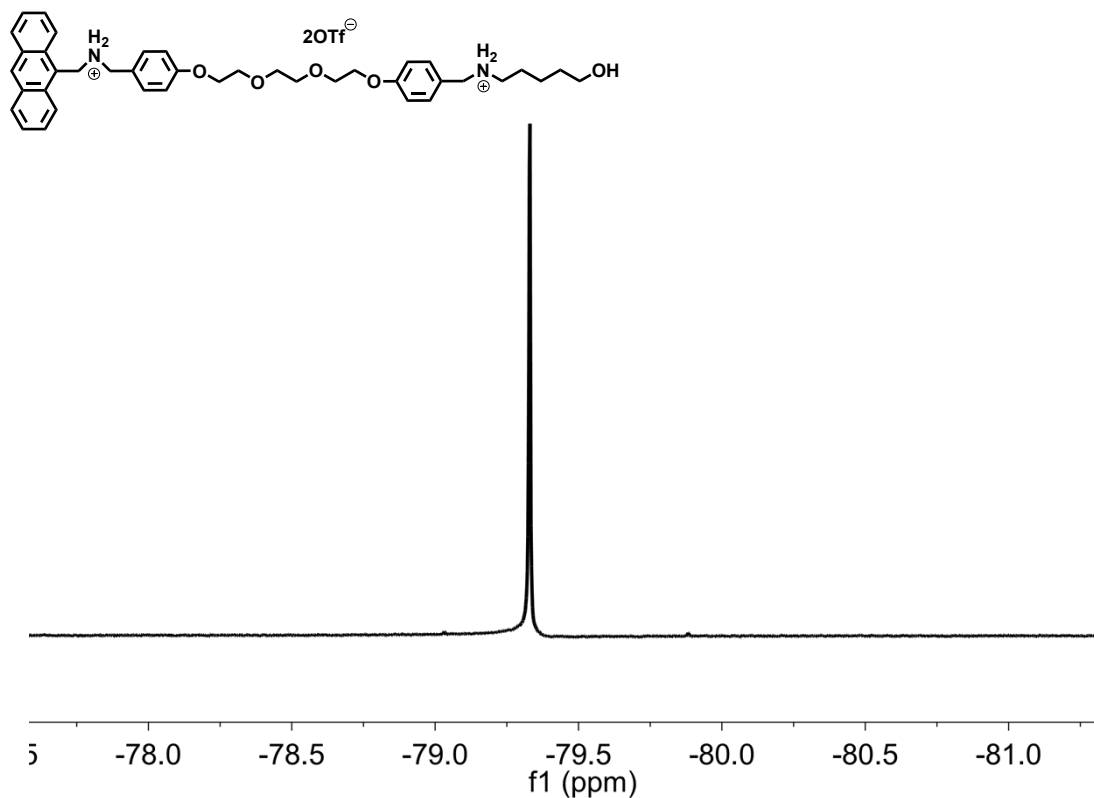


Fig. S3  $^{19}\text{F}$  NMR (400 MHz,  $\text{CD}_3\text{CN}$ , 298K) spectrum of guest 4.

(d)

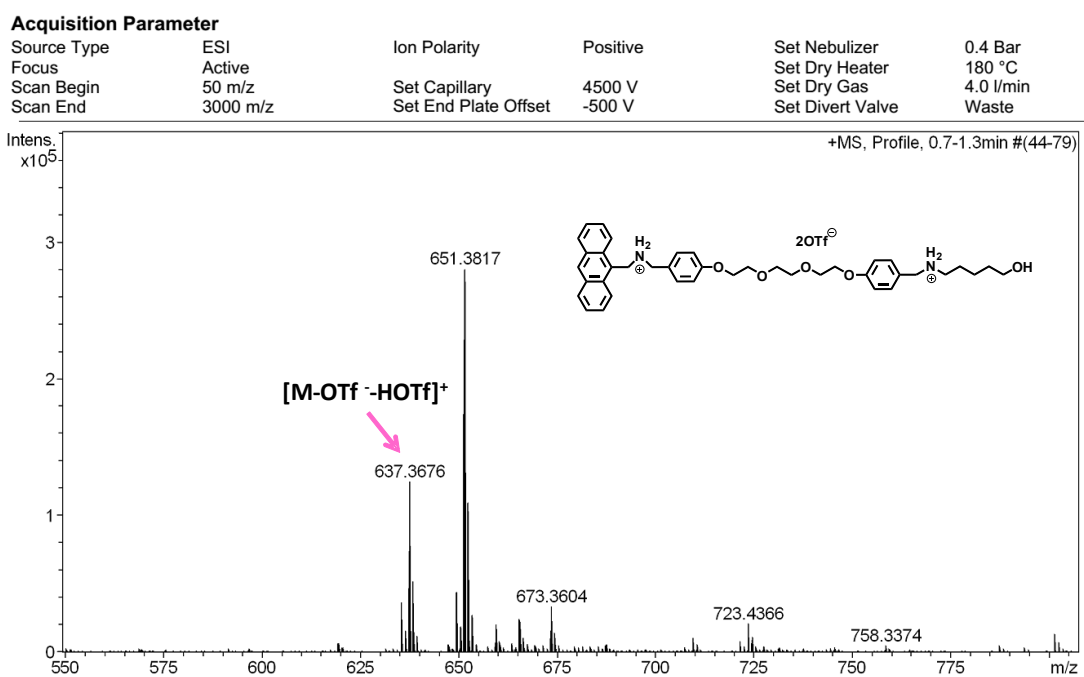
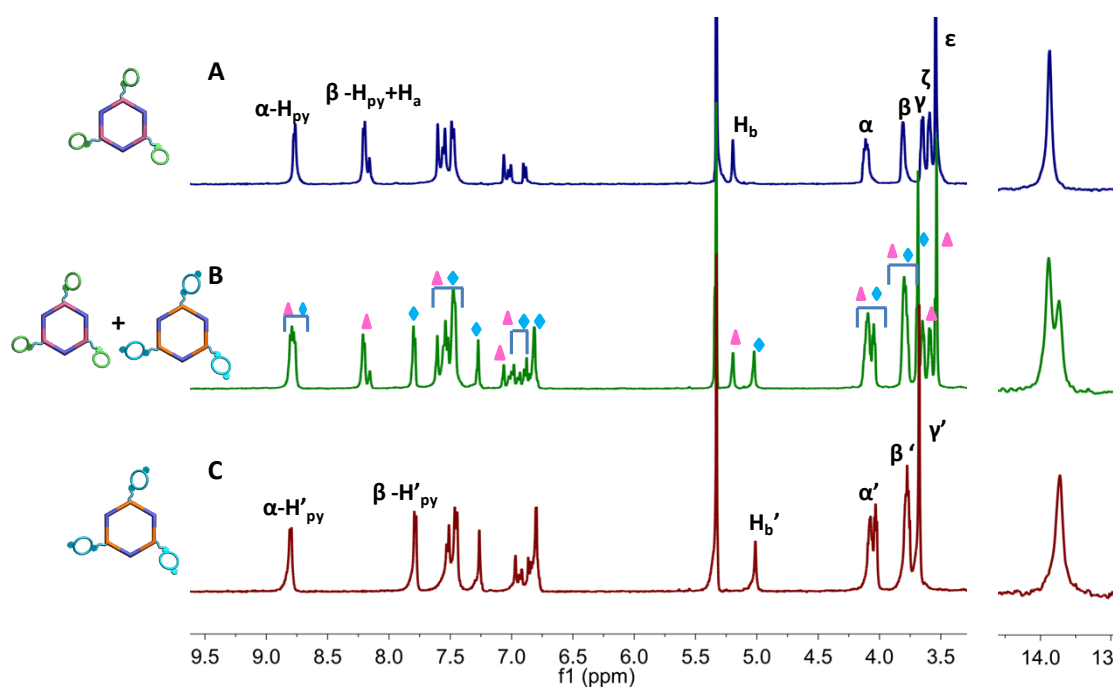


Fig. S4 HRMS (ESI) of 4: Exact mass calcd for  $[\text{C}_{40}\text{H}_{49}\text{N}_2\text{O}_5]^+$ : 637.3636, Found: 637.3676.

### 3. Experimental details of Size-Controlled Self-Sorting Process

**Scheme S2.** Schematic representation of the synthetic procedures for two discrete metallacycles.

**Size-Controlled Self-Sorting Process:** To a mixture of 120° crown ether containing building blocks **1** (1.51 mg, 0.0024 mmol), **2** (1.85 mg, 0.0024 mmol), and 120° di-Pt(II) acceptor **3** (6.56 mg, 0.0049mmol) in a small vessel was added 0.45 mL(CD<sub>2</sub>Cl<sub>2</sub>/CD<sub>3</sub>COCD<sub>3</sub> (2/1,v/v)) solution drop by drop with continuous stirring. The reaction mixture was stirred for another 5 minutes at room temperature and employed for the further characterizations directly.



**Fig. S5** Partial <sup>1</sup>H NMR (400 MHz, CD<sub>2</sub>Cl<sub>2</sub>/CD<sub>3</sub>COCD<sub>3</sub>(2/1), 298K) (left) and <sup>31</sup>P NMR (161.9MHz, CD<sub>2</sub>Cl<sub>2</sub>/CD<sub>3</sub>COCD<sub>3</sub>(2/1), 298K) (right) spectra of (A) the individual metallacycle **5**; (B) the self-sorting system; (C) the individual metallacycle **6**.

#### **4. The construction and characterization of cross-linked supramolecular polymers through self-sorting complexation**

**Scheme S3.** Schematic representation of the synthetic procedures for cross-linked supramolecular polymers.

##### **The construction of four-component supramolecular polymers: *Method I (the stepwise fashion):***

The mixture of above-mentioned crown ether containing building blocks **1**, **2** and **3** were mixed in CD<sub>2</sub>Cl<sub>2</sub> (0.3mL) in a small vessel, then stirring at room temperature to afford two different-sized metallacycles **5** and **6**. Sequentially, the CD<sub>3</sub>COCD<sub>3</sub> (0.15mL) solution of guest **4** (0.91 mg, 0.00290 mmol) was added drop by drop with continuous stirring. After the complexation mixture was stirred for 5 minutes at room temperature, the resultant multicomponent supramolecular system was obtained, which was used for the further characterizations directly.

##### **The construction of four-component supramolecular polymers: *Method II (the one-pot fashion):***

The mixture of above-mentioned four building blocks **1**, **2**, **3** and **4** were mixed in CD<sub>2</sub>Cl<sub>2</sub>/CD<sub>3</sub>COCD<sub>3</sub> (0.3 mL/ 0.15mL, v/v) in a small vessel. After the complexation mixture was stirred for 5 minutes at room temperature, the resultant multicomponent supramolecular system was obtained, which was used for the further characterizations directly.



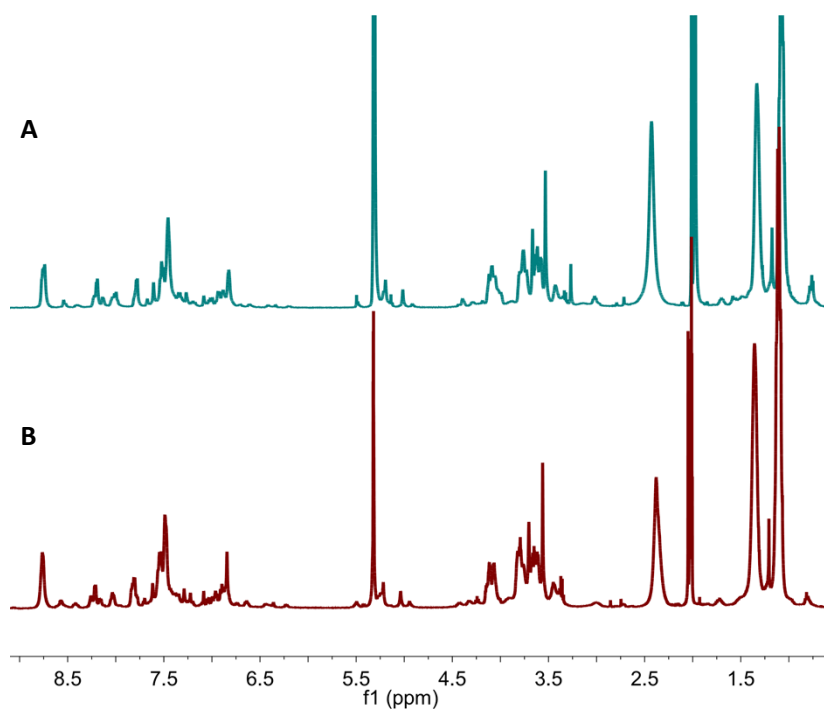


**Fig. S6** Partial  $^1\text{H}$  NMR (500 MHz,  $\text{CD}_2\text{Cl}_2/\text{CD}_3\text{COCD}_3$  (2/1), 298K) spectra of the supramolecular polymer system constructed from (A) stepwise approach; (B) the one-pot approach.

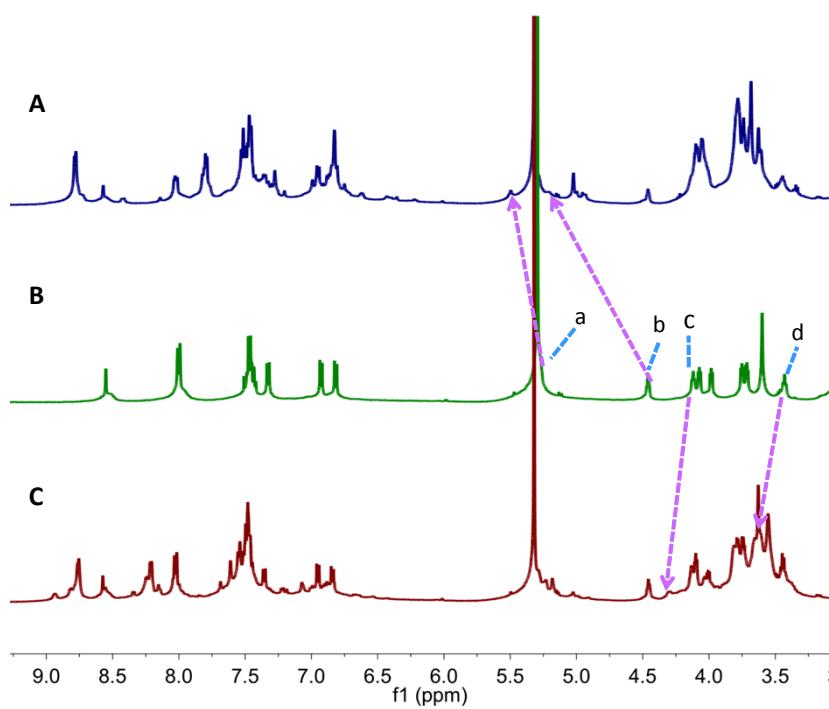


**Fig. S7** Partial  $^1\text{H}$  NMR (500 MHz,  $\text{CD}_2\text{Cl}_2/\text{CD}_3\text{COCD}_3$  (2/1), 298K) spectra of (A) the three-component (2, 3 and 4) complex system; (B) the ditopic guest 4 itself; (C) the three-component (1,

3 and 4) complex system.

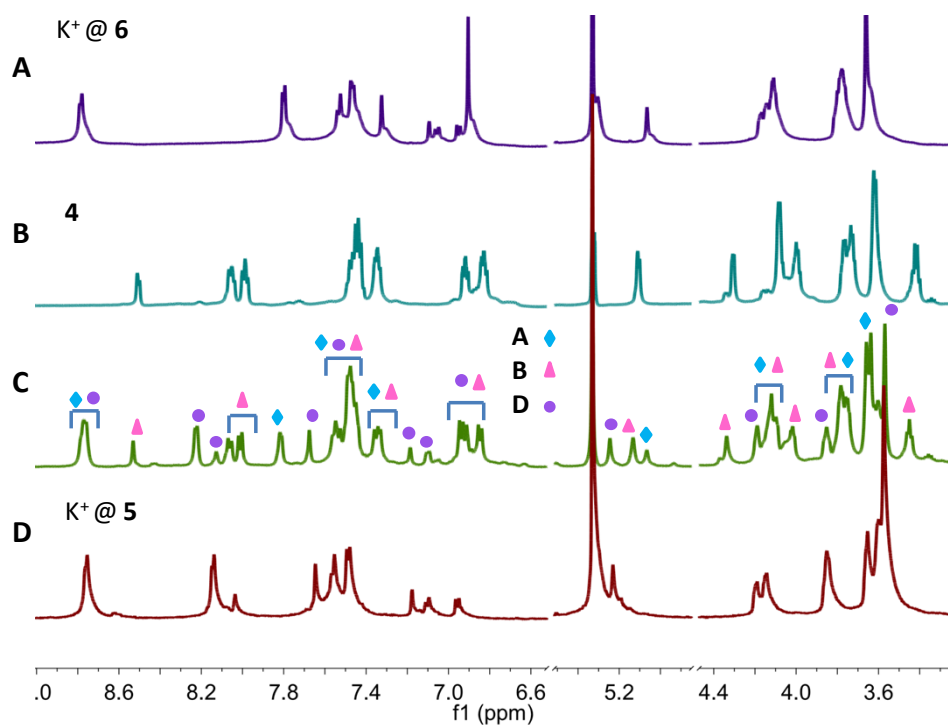


**Fig. S8** Partial <sup>1</sup>H NMR (500 MHz, CD<sub>2</sub>Cl<sub>2</sub>/CD<sub>3</sub>COCD<sub>3</sub> (2/1), 298K) spectra of the (A) K<sup>+</sup> @ 6 complex system, (B) guest 4, (C) after addition of excess KPF<sub>6</sub> to the four-component complex system, (D) K<sup>+</sup> @ 5 complex system.

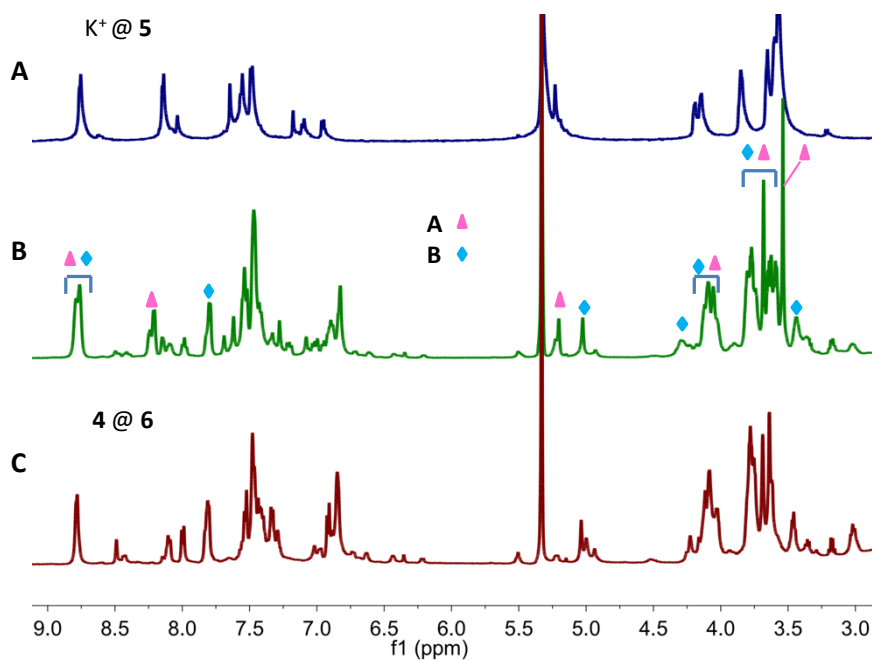


**Fig. S9** Partial <sup>1</sup>H NMR (500 MHz, CD<sub>2</sub>Cl<sub>2</sub>/CD<sub>3</sub>COCD<sub>3</sub> (2/1), 298K) spectra of the (A) K<sup>+</sup> @ complex system; (B) after addition of 1.0 eq. KPF<sub>6</sub> to the four-component complex system; (C)

4 @ 6 complex system.

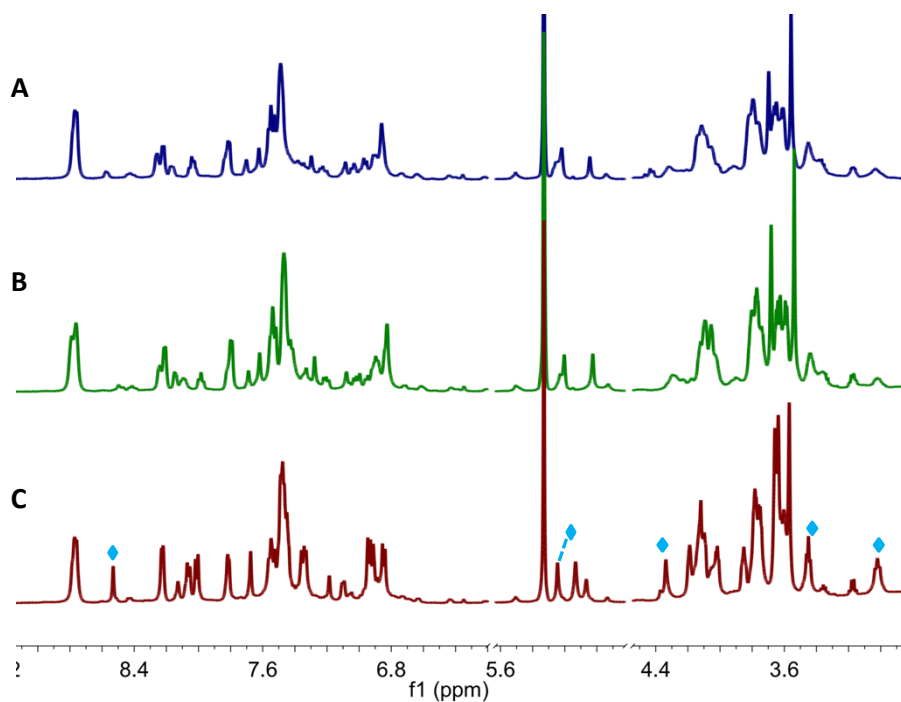


**Fig. S10** Partial  $^1\text{H}$  NMR (500 MHz,  $\text{CD}_2\text{Cl}_2/\text{CD}_3\text{COCD}_3$  (2/1), 298K) spectra of the (A) four-component complex system; (B) after the addition of 1.0 eq.  $\text{KPF}_6$  to the four-component complex system; (C) after subsequent addition of excess  $\text{KPF}_6$  to the four-component complex system.

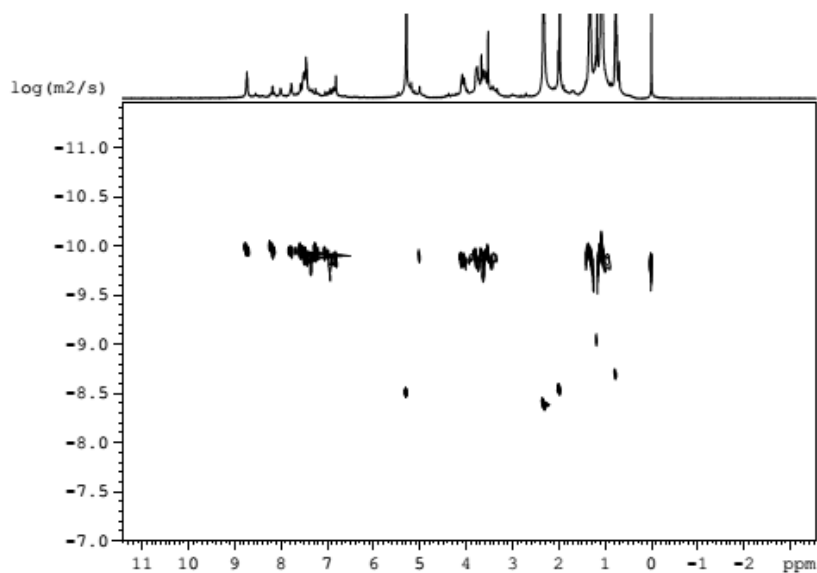


**Fig. S11** DOSY spectrum of supramolecular polymers at concentrations of 1.2 mM guest unit in  $\text{CD}_2\text{Cl}_2/\text{CD}_3\text{COCD}_3$  (2/1, v/v) (500 MHz, 298K).

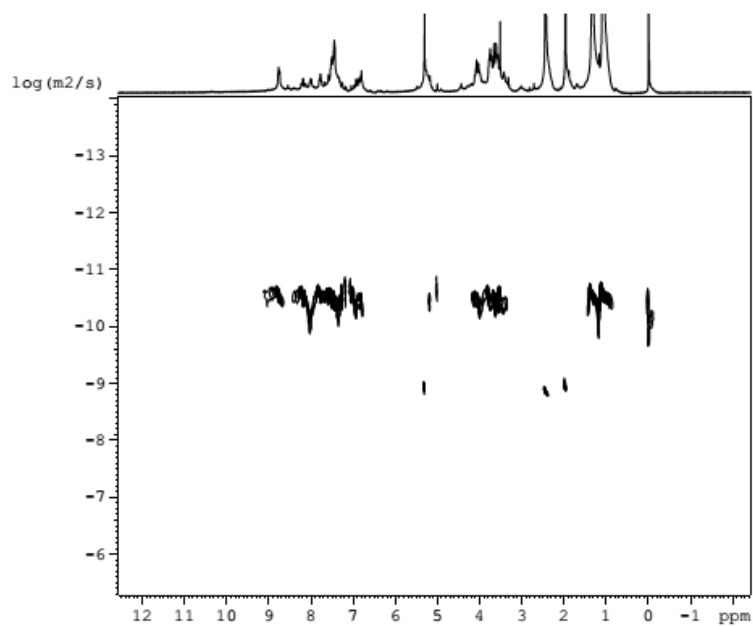


**Fig. S12** DOSY spectrum of supramolecular polymers at concentrations of 2.4 mM guest unit in CD<sub>2</sub>Cl<sub>2</sub>/CD<sub>3</sub>COCD<sub>3</sub> (2/1, v/v) (500 MHz, 298K).

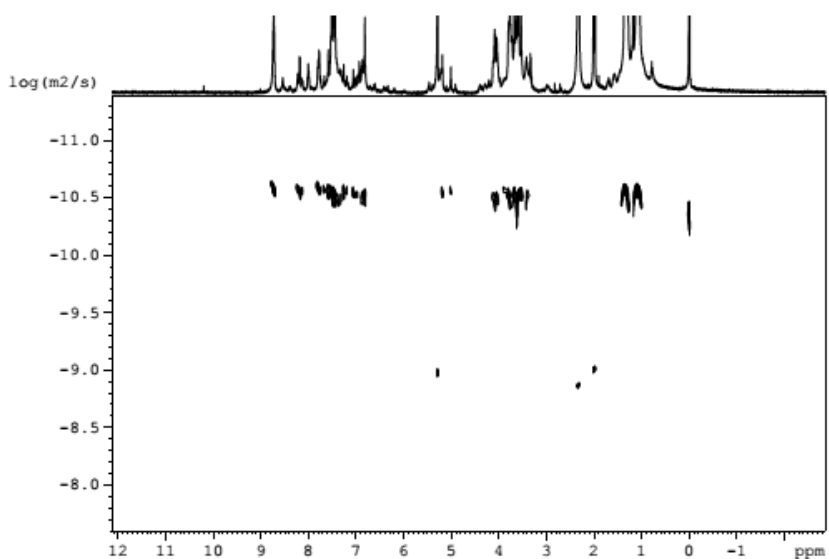


**Fig. S13** DOSY spectrum of supramolecular polymers at concentrations of 3.1 mM guest unit in CD<sub>2</sub>Cl<sub>2</sub>/CD<sub>3</sub>COCD<sub>3</sub> (2/1, v/v) (500 MHz, 298K).

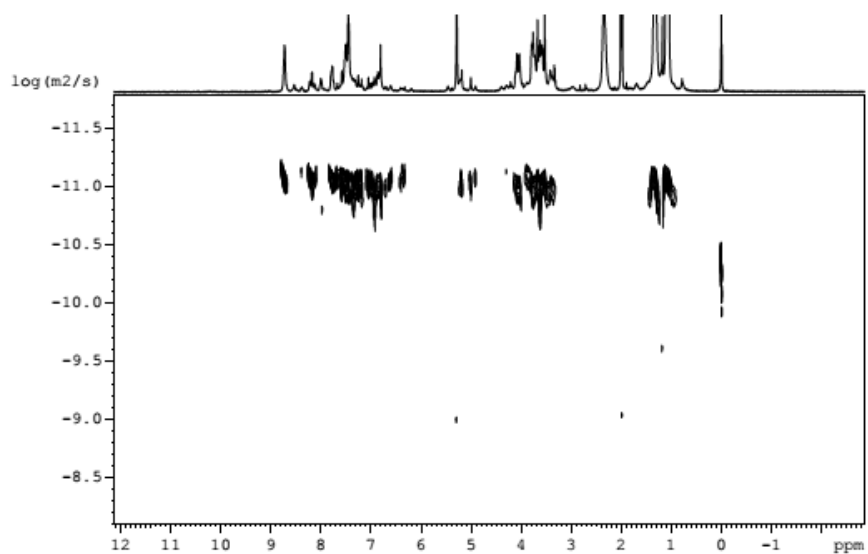


**Fig. S14** DOSY spectrum of supramolecular polymers at concentrations of 4.8 mM guest unit in CD<sub>2</sub>Cl<sub>2</sub>/CD<sub>3</sub>COCD<sub>3</sub> (2/1, v/v) (500 MHz, 298K).

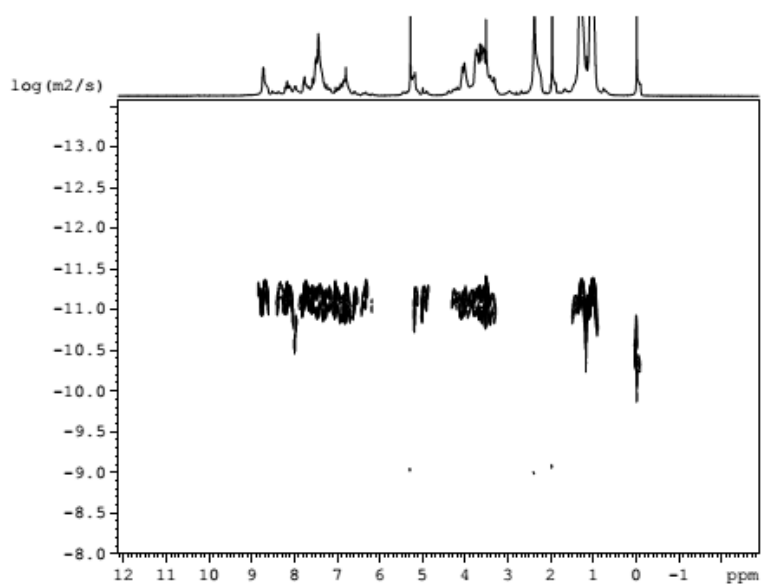


**Fig. S15** DOSY spectrum of supramolecular polymers at concentrations of 5.6 mM guest unit in CD<sub>2</sub>Cl<sub>2</sub>/CD<sub>3</sub>COCD<sub>3</sub> (2/1, v/v) (500 MHz, 298K).

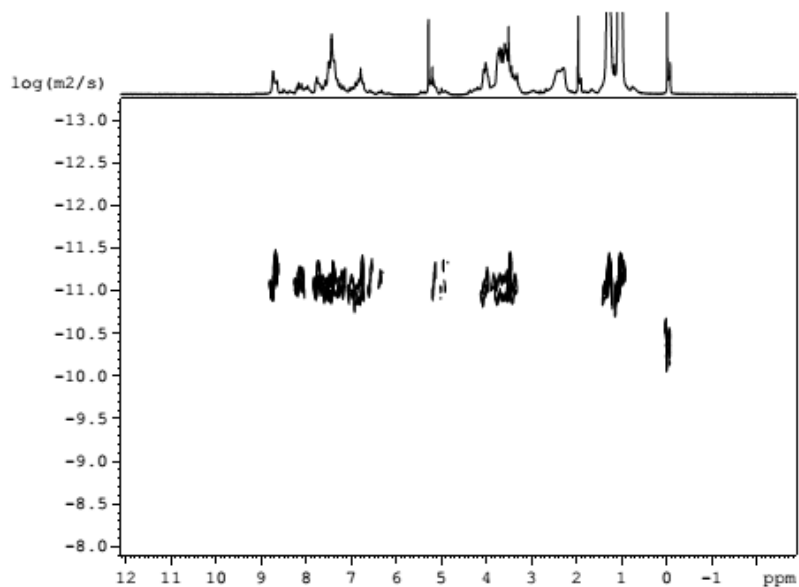


**Fig. S16** DOSY spectrum of supramolecular polymers at concentrations of 8.2 mM guest unit in  $CD_2Cl_2/CD_3COCD_3$  (2/1, v/v) (500 MHz, 298K).

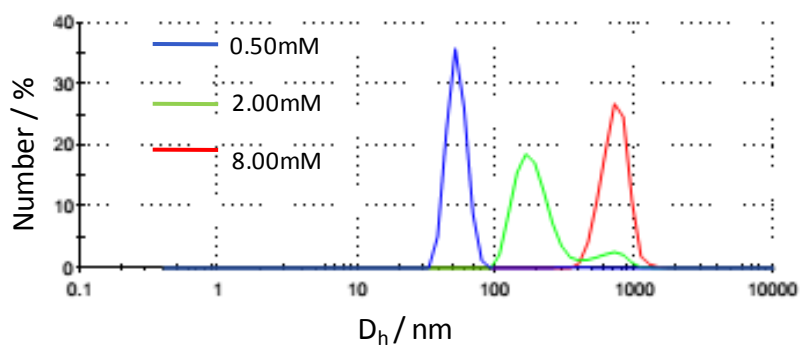


**Fig. S17** DLS data: size distributions of supramolecular polymers at different concentrations.

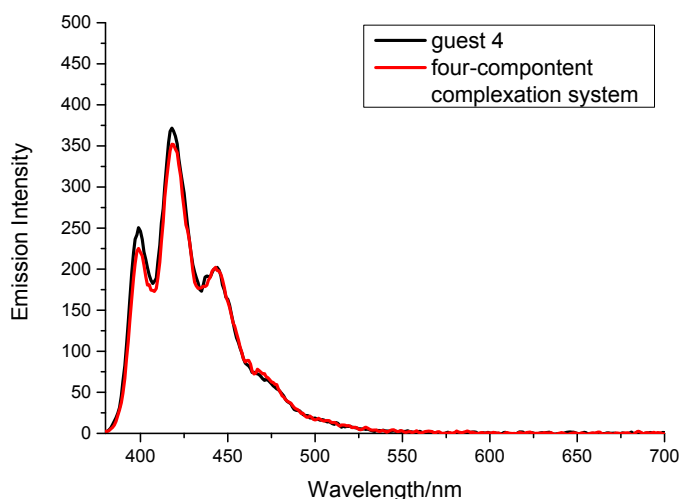


**Fig. S18** Fluorescence emission spectra of ditopic guest **4** and the four-component supramolecular polymer system in the  $\text{CH}_2\text{Cl}_2/\text{CH}_3\text{COCH}_3$  (2/1) mixtures ( $\lambda_{\text{ex}} = 370 \text{ nm}$ ,  $c = 0.1 \text{ mM}$ ).

**The preparation of the SEM samples.** For the samples with low concentration (below 10.0 mM), the samples were drop-casted onto the Si-substrate since the self-sorting supramolecular polymer was in solution. While for the sample with high concentration (above 10.0 mM), the samples were smeared onto the Si-substrate due to the formation of metallogels. Then the samples were prepared by freeze-drying method by using lyophilizer. This approach allowed for maintaining the original morphology preferably, thus avoiding the collapse due to the evaporation of solvent.

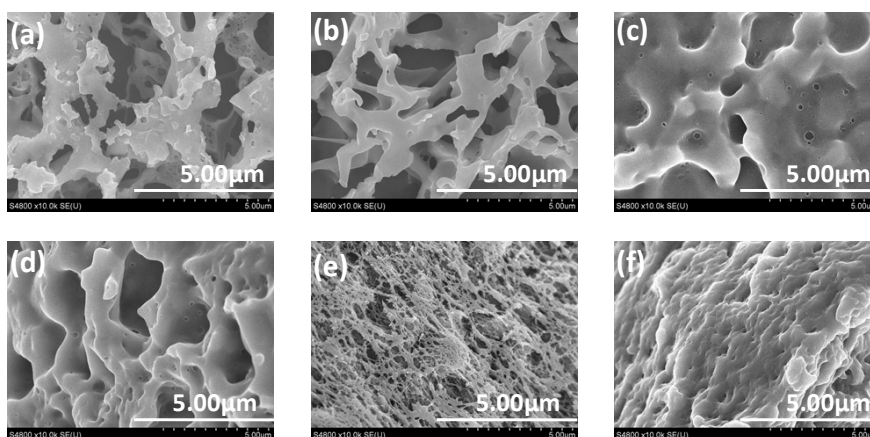


**Fig. S19** Concentration-dependent SEM images of cross-linked supramolecular polymeric system under 5.00  $\mu\text{m}$  scale bars: (a) 1.2 mM; (b) 2.0 mM; (c) 3.2mM; (d) 6.0 mM; (e) 10.0 mM; (f) 18.0 mM.

**The preparation of the TEM samples.** Moreover, concentration-dependent TEM investigation was carried out as well. For the samples with low concentration (below 10.0 mM), the samples were drop-casted on copper grids since the self-sorting supramolecular polymer was in solution. While for the sample with high concentration (above 10.0 mM), the samples were smeared on copper grids due to the formation of metallogels. Then the samples were evaporated in air at room temperature. Notably, for the samples with concentration higher than 10.0 mM, it was very difficult to get good TEM images with high quality, which might be caused by the dense three-dimensional net-works in gel state.

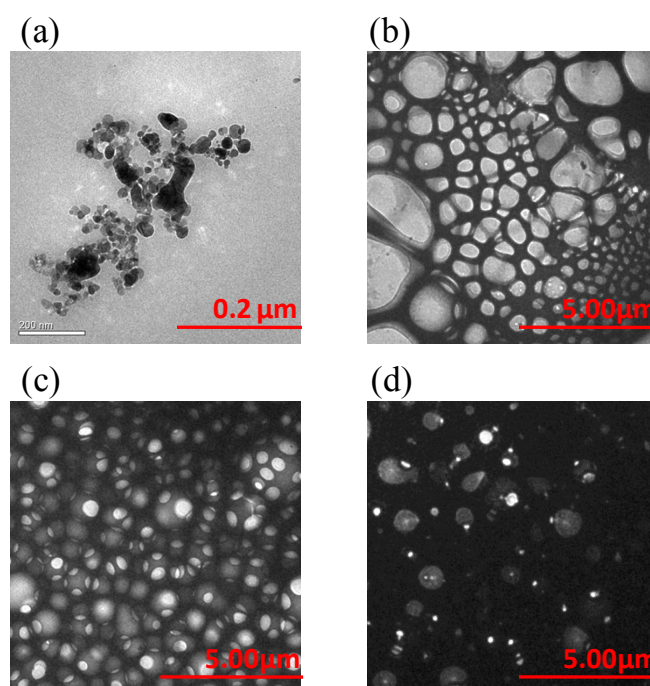


**Fig. S20** Concentration-dependent TEM images of cross-linked supramolecular polymeric system: (a) 1.2 mM; (b) 2.0 mM; (c) 6.0 mM; (d) 10.0 mM.

**Gel ability tests.** The gelation ability of the ditopic guest **4**, the mixture of crown ether containing metallacycles **5** and **6** (in equal ration, similarly hereinafter), the complexation systems of **4** and **B21C7**-containing metallacycle **5** as well as **4** and **DB24C8**-containing metallacycle **6**, and the multicomponent self-sorting polymer systems at the same concentration as the control experiment was investigated. At high concentration (16 mM), only the cross-linked self-sorting supramolecular polymer afforded the formation of stable metallogels, while all other control systems only resulted in the solution without the tendency to gelation. This result clearly proved the crucial roles of the formation of cross-linked self-sorting polymer during the gelation process.



## 5. Stimuli-responsive supramolecular polymer gels

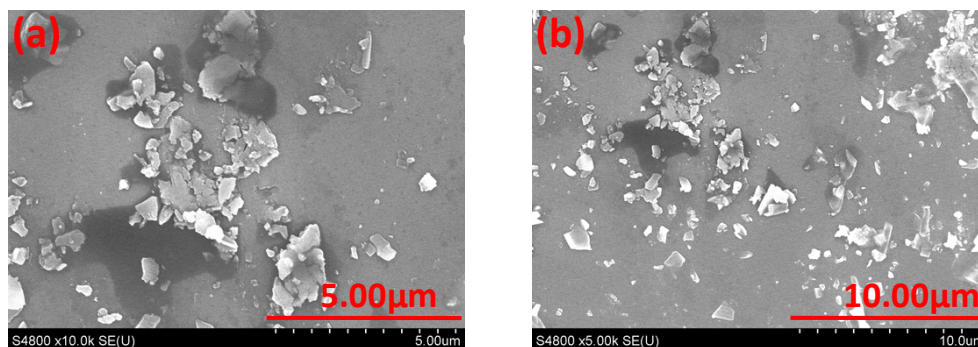


**Fig. S21** SEM images of the destroyed supramolecular gels after addition of  $\text{KPF}_6$  (2.0 eq. relative to the guest unit).

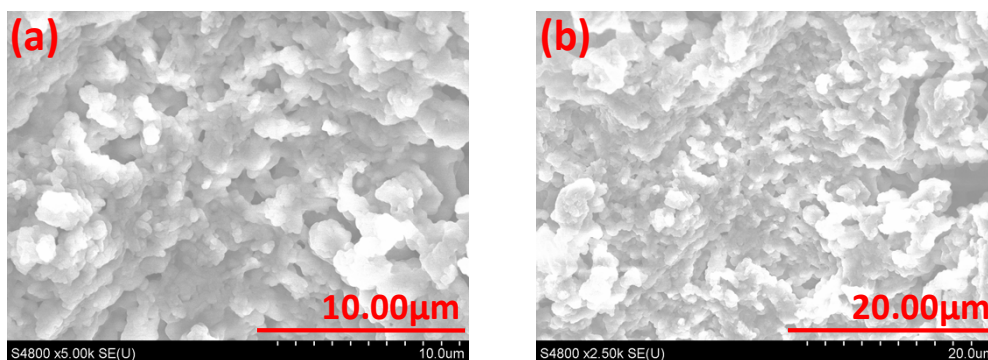


**Fig. S22** SEM images of the reformed supramolecular gels after the subsequent addition of excess  $18\text{C}6$  to the solution.

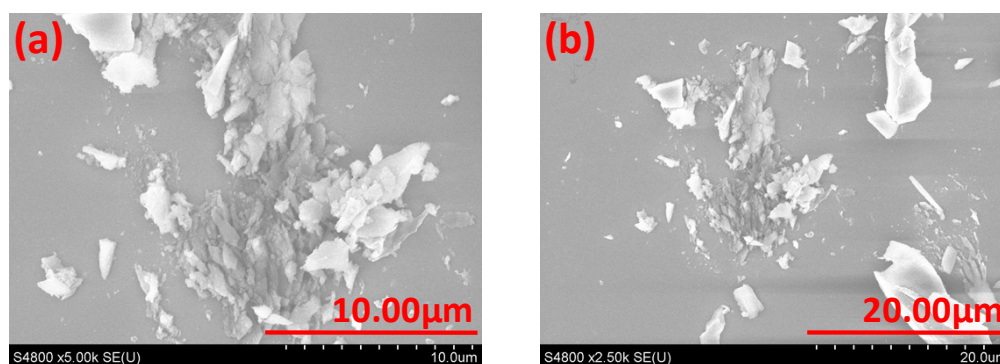


**Fig. S23** SEM images of the destroyed supramolecular gels after addition of TBABr (4.0 eq. relative to the guest unit).

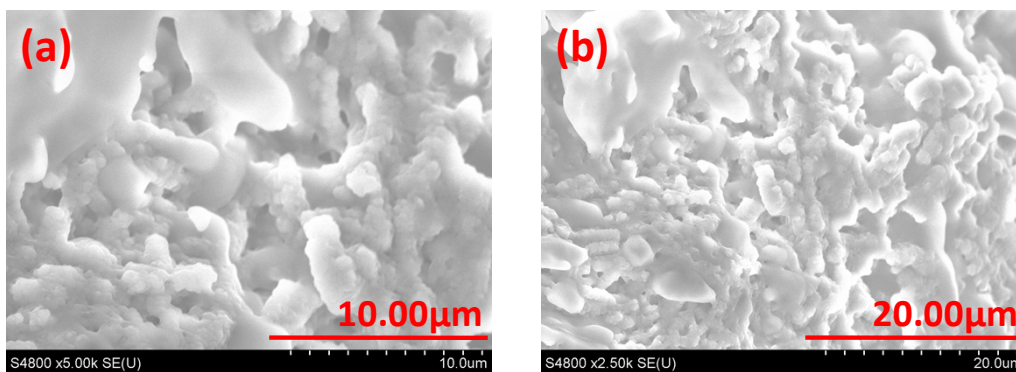


**Fig. S24** SEM images of the reformed supramolecular gels after the subsequent addition of AgOTf to the solution (8.0 eq. to the guest unit).

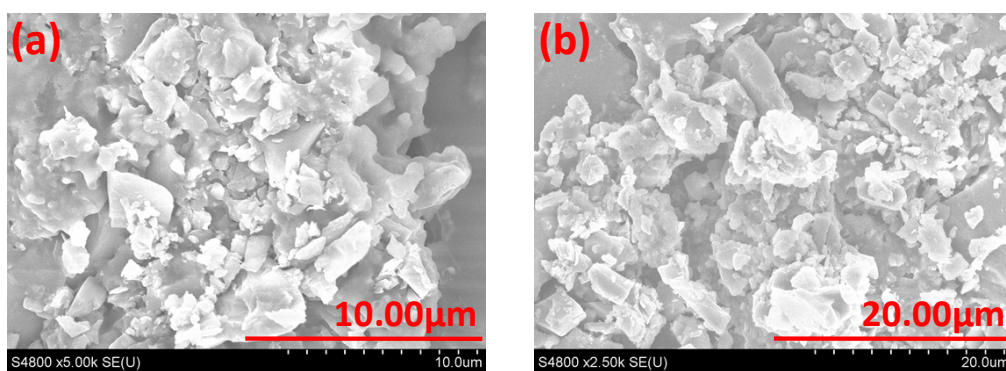


**Fig. S25** SEM images of the destroyed supramolecular gels after addition of Et<sub>3</sub>N(2.0 eq.relative to the guest unit).

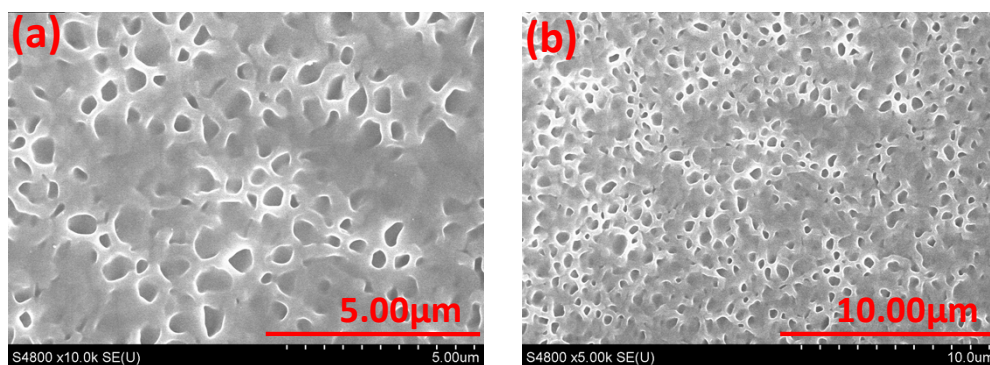


**Fig. S26** SEM images of the reformed supramolecular gels after the subsequent addition of CF<sub>3</sub>COOH to the solution (2.0 eq.relative to the guest unit).

### ***Reference:***

1. W. Wang, Y. Zhang, B. Sun, L.-J. Chen, X.-D. Xu, M. Wang, X. Li, Y. Yu, W. Jiang, H.-B. Yang, *Chem. Sci.*, 2014, **5**, 4554.
2. H.-B. Yang, K. Ghosh, B. H. Northrop, Y.-R. Zheng, M. M. Lyndon, D. C. Muddiman and P. J. Stang, *J. Am. Chem. Soc.*, 2007, **129**, 14187.
3. S. Leininger, M. Schmitz and P. J. Stang, *Org. Lett.*, 1999, **1**, 1921
4. W. Jiang and C. A. Schalley, *Proc. Natl. Acad. Sci. USA*, 2009, **106**, 10425.